

Interaction of N-methyl-2-alkenyl-4-quinolones with ATP-dependent MurE ligase of *Mycobacterium tuberculosis*: antibacterial activity, molecular docking and inhibition kinetics

Juan David Guzman^{1,2}, Abraham Wube³, Dimitrios Evangelopoulos^{1,4}, Antima Gupta¹, Antje Hüfner⁵, Chandrakala Basavannacharya¹, Md. Mukhleshur Rahman², Christina Thomaschitz³, Rudolf Bauer³, Timothy Daniel McHugh⁴, Irene Nobeli¹, Jose M. Prieto², Simon Gibbons², Franz Bucar^{3†} and Sanjib Bhakta^{1‡}

¹Department of Biological Sciences, Institute of Structural and Molecular Biology, Birkbeck College, University of London, Malet Street, London WC1E 7HX, UK; ²Department of Pharmaceutical and Biological Chemistry, The School of Pharmacy, University of London, 29–39 Brunswick Square, London WC1N 1AX, UK; ³Department of Pharmacognosy, Institute of Pharmaceutical Sciences, Karl Franzens University Graz, Universitätsplatz 4, A-8010 Graz, Austria; ⁴Department of Medical Microbiology, Royal Free Hospital, University College London, Rowland Hill Street, London NW3 2PF, UK; ⁵Department of Pharmaceutical Chemistry, Institute of Pharmaceutical Sciences, Karl Franzens University Graz, Universitätsplatz 1, A-8010 Graz, Austria

*Corresponding author. Tel: +44-20-7631-6355/+44-20-7079-0799; Fax: +44-20-7631-6246; E-mail: s.bhakta@bbk.ac.uk

†These authors made an equal contribution to the study.

Received 7 February 2011; returned 18 March 2011; revised 18 April 2011; accepted 27 April 2011

Objectives: The aim of this study was to comprehensively evaluate the antibacterial activity and MurE inhibition of a set of N-methyl-2-alkenyl-4-quinolones found to inhibit the growth of fast-growing mycobacteria.

Methods: Using the spot culture growth inhibition assay, MICs were determined for *Mycobacterium tuberculosis* H₃₇Rv, *Mycobacterium bovis* BCG and *Mycobacterium smegmatis* mc²155. MICs were determined for *Mycobacterium fortuitum*, *Mycobacterium phlei*, methicillin-resistant *Staphylococcus aureus*, *Escherichia coli* and *Pseudomonas aeruginosa* using microplate dilution assays. Inhibition of *M. tuberculosis* MurE ligase activity was determined both by colorimetric and HPLC methods. Computational modelling and binding prediction of the quinolones in the MurE structure was performed using Glide. Kinetic experiments were conducted for understanding possible competitive relations of the quinolones with the endogenous substrates of MurE ligase.

Results: The novel synthetic N-methyl-2-alkenyl-4-quinolones were found to be growth inhibitors of *M. tuberculosis* and rapid-growing mycobacteria as well as methicillin-resistant *S. aureus*, while showing no inhibition for *E. coli* and *P. aeruginosa*. The quinolones were found to be inhibitory to MurE ligase of *M. tuberculosis* in the micromolar range (IC_{50} ~40–200 μM) when assayed either spectroscopically or by HPLC. Computational docking of the quinolones on the published *M. tuberculosis* MurE crystal structure suggested that the uracil recognition site is a probable binding site for the quinolones.

Conclusions: N-methyl-2-alkenyl-4-quinolones are inhibitors of mycobacterial and staphylococcal growth, and show MurE ligase inhibition. Therefore, they are considered as a starting point for the development of increased affinity MurE activity disruptors.

Keywords: 4-quinolones, Mur ligase inhibitors, *M. tuberculosis*

Introduction

Tuberculosis (TB) is a contagious disease caused by infection with species belonging to the *Mycobacterium tuberculosis* complex.¹ This slow-growing acid-fast bacterium exerts a tremendous impact on current global health.² *Staphylococcus aureus* is also

a major concern, as this pathogen is the most common cause of bacterial infection worldwide³ and methicillin-resistant *S. aureus* (MRSA) strains remain difficult to treat,⁴ despite the approval of agents such as linezolid, quinupristin/dalfopristin and daptomycin over the last decade. Infection with drug-resistant *M. tuberculosis* strains is extremely serious, prolonging

© The Author 2011. Published by Oxford University Press on behalf of the British Society for Antimicrobial Chemotherapy.
This is an Open Access article distributed under the terms of the Creative Commons Attribution Non-Commercial License (<http://creativecommons.org/licenses/by-nc/2.5>), which permits unrestricted non-commercial use, distribution, and reproduction in any medium, provided the original work is properly cited.

treatment time, decreasing the probability of cure and increasing the cost of treatment.⁵ The current anti-TB chemotherapy must be administered for 6 months for drug-susceptible strains and for ≥ 2 years for multidrug-resistant (MDR) or extensively drug-resistant (XDR) infections. Outbreaks of drug-resistant pathogens are more and more frequent everywhere, and it would be catastrophic if these pathogens develop total drug resistance.^{6,7} Novel chemical entities are therefore required for treating drug-resistant strains. They must be potent enough to reduce the length of treatment and to prevent the emergence of resistance, but they must also be safer than second-line drugs and not interfere with antiretroviral therapy.⁸ Screening for novel mechanisms of action seems a reasonable strategy to develop inhibitors against MDR, XDR and totally drug-resistant strains of *M. tuberculosis*, as the resulting compounds may have a disrupting effect on pathways or enzymes that have never been targeted before.

Natural products are a primordial source of bioactive chemical scaffolds that have been therapeutically exploited for a large number of diseases.⁹ Plants and microorganisms have developed many successful secondary metabolites for protection against microbial infection. Antibiotics are, by definition, produced by microorganisms¹⁰ and are one of the most valuable antimicrobial classes, as they gained bacteria-killing competence by targeting essential biochemical pathways through centuries of microbial evolution. β -Lactams, glycopeptides, bacitracin, fosfomycin and cycloserine are all antibiotics targeting the peptidoglycan biosynthetic pathway.¹¹ Peptidoglycan is an essential bacterial cell wall polymer that is responsible for cell shape and serves as containment for cytoplasmic pressure. Because it is a well-validated pathway, there is growing interest in developing small molecule inhibitors that target novel proteins of this biosynthetic route.¹² Mycobacterial peptidoglycan is the sustaining mesh that supports the mycolyl-arabinogalactan complex and is therefore considered an indispensable building block.¹³ Mur ligases are cytoplasmic enzymes that perform the biosynthesis of uridine-diphosphate-N-acetylmuramyl-L-Ala-D-Glu-m-DAP-D-Ala-D-Ala (UDP-MurNAc-pentapeptide) from uridine-diphosphate-N-acetylglucosamine (UDP-NAcGlc).¹⁴ ATP-dependent Mur ligases C, D, E and F are able to sequentially add the amino acids forming the pentapeptide chain, and have been shown to act by a similar mechanism to folylpolyglutamate synthetase.¹⁵ The MurE ligase of *M. tuberculosis* preferentially adds meso-diaminopimelic acid (*m*-DAP) to the γ -carboxyl group of glutamic acid in UDP-MurNAc-L-Ala-D-Glu.^{16,17} Natural product inhibitors have been already reported by us¹⁸ and increasing efforts are being made to develop specific inhibitors of this enzyme.

The approach used in this work was to comprehensively evaluate the bioactivity of five synthetic evocarpine-related quinolones. The compounds belonging to this class have been shown to be effective inhibitors of rapid-growing *Mycobacterium* species.¹⁹ N-methyl-2-alkenyl-4-quinolones were tested against slow- and rapid-growing mycobacterial species (*M. tuberculosis* H₃₇Rv, *Mycobacterium bovis* BCG, *Mycobacterium smegmatis*, *Mycobacterium fortuitum* and *Mycobacterium phlei*). The antibacterial activity was also recorded against two epidemic strains of commonly prevalent MRSA (EMRSA-15 and -16) and two Gram-negative bacteria and the cytotoxicity was evaluated against murine macrophages, in order to assess the specificity of the quinolones in whole cell experiments. In our in-house MurE screening programme of potential inhibitors, these quinolones were

shown to inhibit *M. tuberculosis* MurE ligase activity when assayed colorimetrically. This finding was further confirmed by HPLC quantification of UDP-MurNAc-tripeptide, the product of the MurE reaction. The quinolones were computationally modelled and docked into the published *M. tuberculosis* MurE protein X-ray structure (PDB:2wtz) to propose a probable binding site. The docking results and the competition experiments of quinolone **2** with MurE ligands suggest that they bind to a specific hydrophobic pocket close to the uracil-binding site that could be exploited to generate a novel class of antimycobacterials.

Materials and methods

Reagents

Isoniazid, norfloxacin, kanamycin, resazurin, Tween 80, glycerol, *m*-DAP, ATP, bis-trispropane, magnesium chloride, Luria–Bertani broth, Mueller–Hinton broth, RPMI-1640, L-glutamine, heat-inactivated fetal calf serum, DMSO and ammonium formate were purchased from Sigma-Aldrich. Middlebrook 7H9, Middlebrook 7H10, and oleic acid, albumin, dextrose and catalase supplement (OADC) were obtained from BD Diagnostics. The MurE substrate UDP-MurNAc-L-Ala-D-Glu was purchased from the BaCWN synthetic facility (University of Warwick, UK).

Synthesis of N-methyl-2-alkenyl-4-quinolones 1–5

The N-methyl-2-alkenyl-4-quinolones **1–5** were obtained using a synthetic route recently reported.¹⁹ The quinolone alkaloids with a cis-unsaturated aliphatic side chain (**1** and **2**) were prepared by the reaction of cis-unsaturated methyl ketones with N-methyl isatoic acid anhydride in the presence of lithium diisopropylamide (LDA). Trans- α,β -unsaturated methyl ketones were used to prepare alkaloids **3–5** using the same type of condensation with N-methyl isatoic acid anhydride in the presence of LDA. The identity of the quinolone alkaloids and their corresponding intermediates was confirmed by analysis of 1D- and 2D-NMR spectroscopy and liquid chromatography–electrospray ionization–mass spectrometry data. Spectroscopic data of quinolones **1–5** are provided as Supplementary data at JAC Online.

Bacterial strains and cells

M. tuberculosis H₃₇Rv (ATCC 27294), *M. bovis* BCG (ATCC 35734), *M. smegmatis* mc²155 (ATCC 700084), *M. fortuitum* (ATCC 6841), *M. phlei* (ATCC 11758), *Escherichia coli* JM109 (ATCC 53323), *Pseudomonas aeruginosa* (ATCC 25668) and murine RAW264.7 macrophages (ATCC TIB71) were used in this study. EMRSA-15 and -16 were gifts from Dr Paul Stapleton (School of Pharmacy, University of London, UK). Competent *E. coli* BL21(DE3)pLysS cells (New England Biolabs, UK) were used for overproducing MurE ligase of *M. tuberculosis* H₃₇Rv.

Drug susceptibility

The spot culture susceptibility assay for *M. tuberculosis* H₃₇Rv, *M. bovis* BCG and *M. smegmatis* mc²155 species was performed as described previously.²⁰ Briefly, Middlebrook 7H9 mycobacterial cultures were serially diluted to 10⁵ cfu/mL. A 5 μ L aliquot of the diluted culture (~500 viable cells) was spotted onto 5 mL of solidified Middlebrook 7H10 agar medium, supplemented with 10% (v/v) OADC in a six-well plate containing various concentrations of compounds **1–5**. A negative control containing only DMSO was included in each plate. A six-well plate containing various concentrations of isoniazid was also used as a positive control. Following incubation at 37°C for 2 weeks for slow growers and 3 days for *M.*

smegmatis, the MIC was determined as the concentration at which there was no visible mycobacterial growth. Microdilution-based methods using Mueller–Hinton broth for *S. aureus*, and Luria–Bertani broth for *E. coli* and *P. aeruginosa* were employed for the MIC determination of the quinolones.¹⁸ Kanamycin and norfloxacin were used as positive controls. Susceptibilities of *M. fortuitum* and *M. phlei* were assessed as reported previously²¹ in a microdilution assay in cation-adjusted Mueller–Hinton broth using isoniazid as a positive control.

Cytotoxicity towards RAW264.7 macrophages

RAW264.7 macrophages (National Collection of Type Cultures) were maintained in RPMI-1640 medium supplemented with 2 mM L-glutamine and 10% heat-inactivated fetal calf serum, in a humidified incubator containing 5% CO₂, at 37°C, and passaged twice before the assay. The cell suspension was adjusted to 5×10⁵ cells/mL and the assay was performed in 96-well cell culture flat-bottom plates (Costar 3596; VWR) in triplicate. Firstly, 2 µL of the 10 g/L stock solution of compounds **1–5** was added to 200 µL of RPMI-1640 medium in the first row and then 2-fold serially diluted. In each well, 100 µL of diluted macrophage cells was added. After 48 h of incubation, the monocytes were washed twice with PBS and fresh RPMI-1640 medium was added. The plates were then revealed with 30 µL of a freshly prepared and filter-sterilized aqueous 0.01% resazurin solution, and incubated overnight at 37°C. The following day, fluorescence was measured at 590 nm with excitation at 560 nm using a Fluostar Optima microplate reader (BMG LABTECH).

MurE ligase inhibition assay

The MurE protein of *M. tuberculosis* was overexpressed in *E. coli* BL21(DE3)pLysS and purified as previously reported.^{17,18} The phosphate colorimetric detection method was performed for the preliminary screen of the small molecules. Additionally, *M. tuberculosis* MurE inhibition was assayed using HPLC analysis. A solution containing 25 mM bis-trispropane buffer (pH 8.5), 5 mM MgCl₂, 100 µM UDP-MurNAc-dipeptide, 250 µM ATP and 1 mM m-DAP was prepared in water as the enzyme–substrate mixture. Quinolones **1–5** were dissolved in DMSO at a concentration of 25, 8.3, 2.5, 0.83, 0.25 and 0.083 mM, and 2 µL was dispensed into 0.5 mL Eppendorfs. MurE enzyme was added to the enzyme–substrate mixture at a final concentration of ~40 nM, and 48 µL of the mixture was rapidly added to each Eppendorf and incubated at 37°C for 30 min. The reaction was stopped by denaturing the protein at 100°C using a block heater for 10 min. The content was centrifuged for homogenization at 4000 rpm for 30 s and then transferred to 200 µL glass inserts (Supelco) fitted to HPLC vials that were analysed directly by HPLC (Agilent 1100 series) using an octadecylsilane RP-18 column (4.6 mm×250 mm×5 µm, Jones chromatography) eluting isocratically with a buffer of 50 mM ammonium formate (pH 4.0) and at a flow rate of 0.5 mL/min. The products of the reaction were detected at 268 nm and 220 nm simultaneously using a diode array detector system. A calibration curve was constructed for the tripeptide and confirmed a good linearity ($R^2=0.9978$) of the signal at 268 nm to the concentration of UDP-MurNAc-tripeptide. Activity controls at 0% (without enzyme) and 100% (with enzyme) were included.

Docking the MurE protein structure

The protein was prepared using the protein preparation wizard of the Maestro software (Schrödinger Software Suite 2009) from the PDB:2wtz file downloaded from the RCSB Protein Data Bank web site (<http://pdb.org/pdb/explore/explore.do?structureId=2wtz>). Chain B was selected and the peptide plane of Thr-298 was rotated to prevent overlapping with His-307. All of the residues were left charged as expected at a working pH of 8.5, except for Glu-198, which was set uncharged. The

modified residue N6-carboxylsine-262 was appropriately recognized. The docking grid was built as a centroid of 30 Å, choosing the residues fundamental for the binding of the substrate according to the PDBsum LigPlot diagram,²² such as Ala-69, Thr-85, Thr-86, Thr-195, Glu-198, Ser-222 and His-248. The ligands **1–5** were drawn using Chemdraw, converted into sdf format with BabelGUI and, lastly, were all processed using LigPrep at pH 8.5±1.0. Docking was performed with Glide²³ using standard precision scoring and varying amide bond conformations.

Kinetic competition assays

Different concentrations of **2** (1000, 300, 100, 30 and 0 µM) were prepared separately with different concentrations of the MurE substrates: UDP-MurNAc-dipeptide (300, 100, 30, 10 and 3 µM); m-DAP (300, 100, 30, 10 and 3 µM); and ATP (300, 100, 30, 10 and 3 µM). The formation of the UDP-MurNAc-tripeptide product was followed by HPLC after 30 min of reaction. The conditions of the reaction and the analytical system were exactly the same as those described earlier for the HPLC inhibition assay. The experiments were performed in duplicate, and the total amount formed was calculated from the area under the peak (retention time ~7 min) using the calibration curve and divided by the time (30 min) to obtain the velocity in µM/min.

Results

Bacterial growth inhibition and cytotoxicity

All of the synthesized N-methyl-2-alkenyl-4-quinolones (**1–5**) (Figure 1a) were significantly active in susceptibility testing on rapid-growing mycobacteria. They also showed growth inhibition of slow-growing mycobacteria (*M. tuberculosis* H₃₇Rv and *M. bovis* BCG), having an MIC value between 5 and 25 mg/L (Table 1). The quinolones were more active against rapid-growing species, showing an MIC value between 0.5 and 10 mg/L. The growth of the highly problematic EMRSA strains was also notably inhibited, revealing MIC values in the range of 0.5–4 mg/L. Moreover, the quinolones did not show any significant inhibition at 50 mg/L for *E. coli*, behaving similarly to the control, isoniazid. The MIC values of **1–5** for *E. coli* were >1000 mg/L and for *P. aeruginosa* they were >256 mg/L. These compounds were moderately cytotoxic towards macrophage RAW264.7 cells, having a 50% growth inhibition concentration (GIC₅₀) of between 24 and 112 mg/L (Table 1). The selectivity index (SI), defined as the GIC₅₀ value divided by the MIC, varied between 1.0 and 5.6 for *M. tuberculosis*, but was much higher for *S. aureus* (SI: 9.75–112).

M. tuberculosis MurE ligase inhibition

MurE ligase activity in the presence of compounds was assayed by HPLC quantification of the product (UDP-MurNAc-L-Ala-D-Glu-m-DAP) formed after 30 min and by the phosphate colorimetric detection method. Clearly, all of quinolones **1–5** showed inhibition of MurE [Figures 1b and S1 (Figure S1 is available as Supplementary data at JAC Online)], displaying an IC₅₀ value of 95–207 µM when determined by HPLC and of 36–72 µM when analysed by the phosphate detection colorimetric method (Table 1). Quinolone **2** was the most active MurE inhibitor, with an IC₅₀ value of 95 µM, as can be inferred from the chromatograms at different concentrations of the inhibitor (Figure 1b). The difference between the MurE inhibition values determined

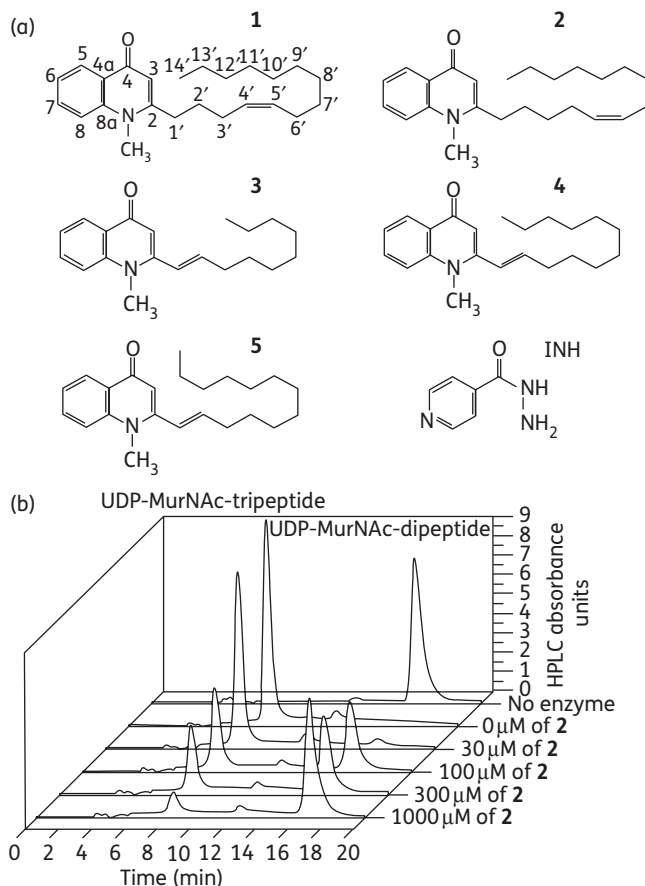


Figure 1. Structure of *N*-methyl-2-alkenyl-4-quinolones **1–5** and isoniazid (INH), and HPLC MurE inhibitory activity of quinolone **2**. (a) Chemical structure of the synthesized quinolones showing the modifications on the alkenyl chain. (b) HPLC chromatograms at 268 nm of the product (UDP-MurNAc-tripeptide) and the substrate (UDP-MurNAc-dipeptide) of the reaction catalysed by *M. tuberculosis* MurE in the presence of different concentrations of quinolone **2**.

by the phosphate and HPLC methods had a consistent value for all of the quinolones.

Docking of the quinolones in the MurE structure

The MurE substrate UDP-MurNAc-L-Ala-D-Glu used as a self-dock test²³ was effectively docked in the same orientation as the published MurE-substrate crystal structure (PDB:2wtz), displaying a GlideScore of -9.92 kcal/mol . The root mean square distance of the heavy atoms of the UDP-MurNAc-L-Ala-D-Glu substrate in the docked and crystal structures was 3.09 \AA , indicating a good preparation of the protein and adequate docking parameters. Our results suggested that all of the quinolones interacted in a similar fashion to a pocket located near the uracil recognition site (Figure 2a) of the Rossmann fold in domain 1 of MurE.¹⁴ According to the calculated hydrophilicity surface of the protein (Figure 2b), the quinolone was attracted to the lipophilic patches on the protein surface. The GlideScore for quinolones **1–5** was in the range of -2.46 to -4.51 kcal/mol , with quinolone **4** having the highest score in absolute value. This

range indicated a rather weak binding, as can be observed in the orientations with a single hydrogen bond participating in the interaction (via the hydroxyl group of Thr-176 to the tertiary nitrogen atom of the quinolone in Figure 2c).

Kinetic competition between the quinolones and MurE substrates

The velocity of formation of the MurE product in the presence of quinolone **2** displayed a dependence on the concentration of the UDP-MurNAc-dipeptide substrate. At a high concentration of UDP-MurNAc-dipeptide (300 and $100\text{ }\mu\text{M}$), the velocity decreased with an increase in the concentration of the quinolone (Figure 3a). For these two concentrations, the fitted lines converge to a point of intersection, therefore indicating competitive inhibition between the UDP-MurNAc-dipeptide and the quinolone.²⁴ However, at a low concentration of UDP-MurNAc-dipeptide (30 , 10 and $3\text{ }\mu\text{M}$), the velocity of MurE product formation was independent of the concentration of the quinolone. For the two other substrates, namely ATP (Figure 3b) and *m*-DAP (Figure 3c), the change in the velocity was less drastic when varying the concentration of the quinolone, and the curves had the same tendency without converging to a point of intersection, indicating uncompetitive inhibition.²⁴

Discussion

Initially isolated as the active antimycobacterial entities from the fruits of the traditional Chinese medicinal tree *Evodia rutaecarpa* (Rutaceae),²⁵ the *N*-methyl-2-alkenyl-4-quinolone chemotype was further exploited by synthetic methods in order to explore chemical variation and improve activity.¹⁹ A group of these chemical entities, which showed the highest activity on rapidly growing mycobacteria, were selected for a comprehensive biological evaluation. We found that these compounds were growth inhibitors of mycobacterial species and the highly problematic EMRSA strains, being also inhibitors of the MurE ligase of *M. tuberculosis*. The MIC indicated that these compounds are notable antibacterials, particularly against EMRSA-15 and -16, which are regularly encountered in UK hospitals.²⁶ The macrophage SI in relation to the *H37Rv* strain for the quinolones was considerably low ($\text{SI} < 10$);²⁷ however, the SI in relation to EMRSA-15 and -16 was much higher (SI range 9.75 – 112), indicating a promising selectivity. Moreover, the compounds did not show inhibition of *E. coli* growth up to a high dose and they are probably innocuous to bacterial gut flora. It was also noted that the cytotoxicity was reduced when the linear alkenyl chain was extended, suggesting an interesting relation for differential selectivity.

The 4-quinolone nucleus is a specific class of compound that has attracted and continues to attract significant interest from the pharmaceutical industry, principally because of the impact of the fluoroquinolones, which inhibit both DNA gyrase and topoisomerase IV,²⁸ and the anticancer 2-phenyl-4-quinolones targeting tubulin.²⁹ In comparison to the fluoroquinolones, the compounds of the present study lack a carboxyl group at position C-3, which is considered to be essential for DNA gyrase inhibition,³⁰ and therefore a further mechanism of action must be assumed. Moreover, this class of chemicals may also be

Table 1. MICs for different species of bacteria, GIC₅₀ and SI for macrophage cells and MurE IC₅₀ of the synthetic quinolones **1–5**

Compound	MIC in mg/L (μ M)						Murine macrophages		M. tuberculosis MurE		
	<i>S. aureus</i>								IC ₅₀ (μ M)		
	<i>M. tuberculosis</i> H ₃₇ Rv	<i>M. bovis</i> BCG	<i>M. smegmatis</i> mc ² 155	<i>M. fortuitum</i>	<i>M. phlei</i>	EMRSA-15	EMRSA-16	GIC ₅₀ (mg/L)	SI	phosphate-based method	HPLC method
1	25 (70.7)	10 (28.3)	10 (28.3)	0.5 (1.41)	0.5 (1.4)	1 (2.8)	0.5 (1.4)	24 ± 9	1.0	52 ± 22	159 ± 6
2	10 (28.3)	10 (28.3)	10 (28.3)	1 (2.83)	1 (2.8)	1 (2.8)	0.5 (1.4)	39 ± 12	3.9	36 ± 16	95 ± 9
3	25 (84.0)	25 (84.0)	5 (16.8)	2 (6.72)	1 (3.4)	4 (13.4)	2 (6.72)	39 ± 11	1.6	70 ± 25	207 ± 6
4	10 (30.7)	5 (15.3)	5 (15.3)	1 (3.06)	0.5 (1.5)	2 (6.12)	2 (6.12)	40 ± 7	4.0	72 ± 23	187 ± 8
5	20 (58.9)	10 (29.4)	10 (29.4)	1 (2.94)	1 (2.9)	2 (5.8)	1 (2.9)	112 ± 10	5.6	52 ± 20	140 ± 5
Isoniazid	0.1 (0.73)	0.1 (0.73)	5 (18.5)	1 (3.65)	4 (15)	ND	ND	>500	>5000	>1000	>1000

ND, not determined.

The MIC of norfloxacin was 0.5 and 256 mg/L for EMRSA-15 and -16, respectively.

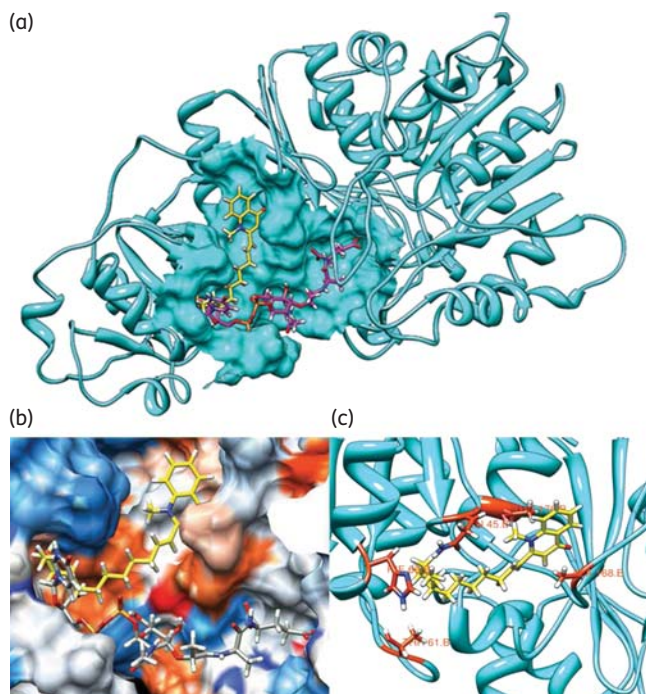
The SI was calculated by dividing the GIC₅₀ by the MIC for *M. tuberculosis* H₃₇Rv.IC₅₀ and GIC₅₀ values are shown ± SD.

Figure 2. Lowest GlideScore docking pose of quinolone **4** interacting with MurE (PDB:2wtz) of *M. tuberculosis*.¹⁷ (a) Presumed binding pocket of the quinolones (in yellow) near the uracil recognition site of UDP-MurNAc-dipeptide (in magenta). (b) Protein surface showing the high hydrophobicity (in red) of the quinolone binding pocket calculated using UCSF Chimera software.³⁴ (c) MurE residues that may interact with the quinolones: Thr-176, Ala-168, Gln-45, His-66 and Thr-61. This figure appears in colour in the online version of JAC, and in black and white in the print version of JAC.

exploited for the discovery and development of bacterial Mur ligase inhibitors. Using both colorimetric and HPLC methods, it was found that the compounds reproducibly inhibited *in vitro* the ligase activity of MurE from *M. tuberculosis*. Comparing **1** and **2**, a slight influence on MurE inhibition was observed for the position of the double bond in the alkenyl chain. Furthermore, the percentage of inhibition when determined using the phosphate colorimetric method was slightly higher than when compared with the HPLC method, probably because of a small decoupling between phosphatase and ligase activities.

For the computational prediction of the binding of potential ligands to a protein, it is advisable to use a 3D structural model of atomic resolution,³¹ typically below 2 Å. However, in the absence of structures of MurE from *M. tuberculosis* below 2 Å resolution, we used the available published model at 3 Å as a preliminary basis for assessing probable binding sites. Interestingly, quinolones **1–5** were predicted to bind to a hydrophobic pocket located near the uridine recognition site in domain 1 of the enzyme. The GlideScore was low (~−4 kcal/mol) in comparison with general reported values for inhibitors (~−10 kcal/mol);³² however, considering the weak interactions between the quinolones and the protein, it is not surprising to observe low GlideScore values. This also indicates that there is space for improvement in the search for chemical and steric complementarities, and the possibility of using this lipophilic cavity for rational drug design. We hypothesize that the aliphatic lipophilic chain of **1–5** interacts with the buried hydrophobic residues of MurE ligase, probably inducing a change in the conformation that prevents binding to UDP-MurNAc-dipeptide. In order to gain further evidence of this possibility, a kinetic competition experiment showed that at a low concentration of the dipeptide, the velocity of the reaction was unaltered by the concentration of the inhibitor. At low concentration of the dipeptide substrate, the majority of the enzyme was free and,

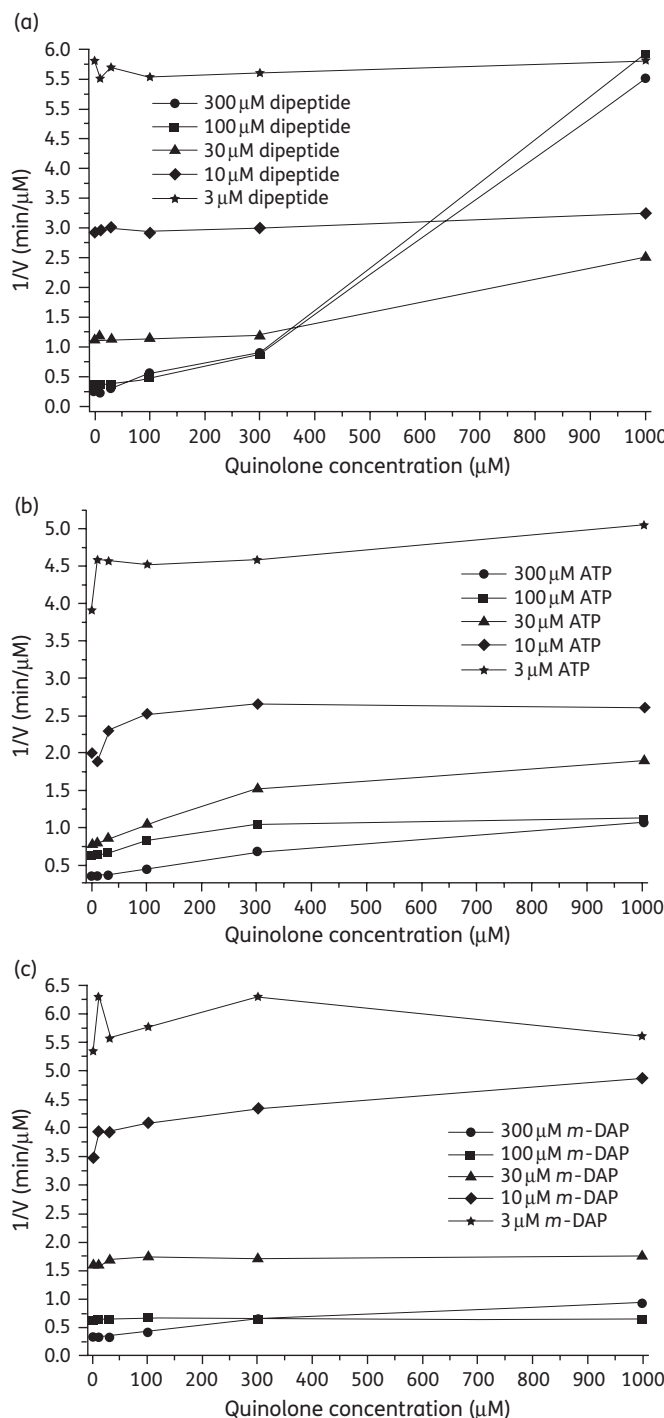


Figure 3. Dixon plots of the activity of the MurE enzyme assayed by HPLC. (a) Plot of the inverse of the velocity of UDP-MurNAc-tripeptide formation versus the concentration of quinolone 2, for different concentrations of UDP-MurNAc-dipeptide. (b) Plot of the inverse of the velocity of UDP-MurNAc-tripeptide formation versus the concentration of quinolone 2, for different concentrations of ATP. (c) Plot of the inverse of the velocity of UDP-MurNAc-tripeptide formation versus the concentration of *m*-DAP.

therefore, according to our results, the conformation of the free MurE enzyme has low interaction with the quinolones. However, when the concentration of the dipeptide substrate was high, most of the enzyme formed the enzyme–substrate complex, which, in agreement with the induced-fit theory,³³ has a different protein conformation. Our results suggested that this induced-fit enzyme–substrate conformation of MurE interacted with the quinolones and when this conformation occurred, inhibition of ligase activity took place. This novel type of MurE inhibitor can be included as a starting point in virtual and fragment screening MurE projects that may help in the detection of structure–activity relationships. Structural modifications of a particularly interesting MurE inhibitor pharmacophore can potentially lead to potent and selective antibacterials in the near future.

Acknowledgements

We thank Dr Philip Lowden (Birkbeck College, London, UK) for support in the HPLC analysis.

Funding

This work was supported by the Medical Research Council, UK (grant G0801956) and the Austrian Science Fund (FWF): project P21152-B18. Colfuturo and Bloomsbury Colleges contributed towards J. D. G.'s research study.

Transparency declarations

None to declare.

Supplementary data

The spectroscopic data of the quinolones 1–5 and Figure S1 are available as Supplementary data at JAC Online (<http://jac.oxfordjournals.org/>).

References

- 1 Cole ST. Comparative and functional genomics of the *Mycobacterium tuberculosis* complex. *Microbiology* 2002; **148**: 2919–28.
- 2 WHO. *Global Tuberculosis Control, WHO Report*. Geneva: WHO, 2010.
- 3 DeLeo FR, Otto M, Kreiswirth BN et al. Community-associated methicillin-resistant *Staphylococcus aureus*. *Lancet* 2010; **375**: 1557–68.
- 4 Howden BP, Ward PB, Charles PGP et al. Treatment outcomes for serious infections caused by methicillin-resistant *Staphylococcus aureus* with reduced vancomycin susceptibility. *Clin Infect Dis* 2004; **38**: 521–8.
- 5 Ormerod LP. Multidrug-resistant tuberculosis (MDR-TB): epidemiology, prevention and treatment. *Br Med Bull* 2005; **73–4**: 17–24.
- 6 Walsh FM, Amyes SGB. Microbiology and drug resistance mechanisms of fully resistant pathogens. *Curr Opin Microbiol* 2004; **7**: 439–44.
- 7 Velayati AA, Farnia P, Masjedi MR et al. Totally drug-resistant tuberculosis strains: evidence of adaptation at the cellular level. *Eur Resp J* 2009; **34**: 1202–3.
- 8 Ginsberg AM, Spigelman M. Challenges in tuberculosis drug research and development. *Nat Med* 2007; **13**: 290–4.

- 9** Newman DJ, Cragg GM. Natural products as sources of new drugs over the last 25 years. *J Nat Prod* 2007; **70**: 461–77.
- 10** Waksman SA. What is an antibiotic or an antibiotic substance? *Mycologia* 1947; **39**: 565–9.
- 11** Silver LL. Does the cell wall of bacteria remain a viable source of targets for novel antibiotics? *Biochem Pharmacol* 2006; **71**: 996–1005.
- 12** Bugg TDH, Braddick D, Dowson CG et al. Bacterial cell wall assembly: still an attractive antibacterial target. *Trends Biotechnol* 2011; **29**: 167–73.
- 13** Hett EC, Rubin EJ. Bacterial growth and cell division: a mycobacterial perspective. *Microbiol Mol Biol Rev* 2008; **72**: 126–56.
- 14** Smith CA. Structure, function and dynamics in the mur family of bacterial cell wall ligases. *J Mol Biol* 2006; **362**: 640–55.
- 15** Bertrand JA, Fanchon E, Martin L et al. ‘Open’ structures of MurD: domain movements and structural similarities with folylpolyglutamate synthetase. *J Mol Biol* 2000; **301**: 1257–66.
- 16** Basavannacharya C, Moody P, Munshi T et al. Essential residues for the enzyme activity of ATP-dependent MurE ligase from *Mycobacterium tuberculosis*. *Protein Cell* 2010; **1**: 1011–22.
- 17** Basavannacharya C, Robertson G, Munshi T et al. ATP-dependent MurE ligase in *Mycobacterium tuberculosis*: biochemical and structural characterisation. *Tuberculosis* 2010; **90**: 16–24.
- 18** Guzman JD, Gupta A, Evangelopoulos D et al. Anti-tubercular screening of natural products from Colombian plants: 3-methoxynordomesticine, an inhibitor of MurE ligase of *Mycobacterium tuberculosis*. *J Antimicrob Chemother* 2010; **65**: 2101–7.
- 19** Wube AA, Hüfner A, Thomaschitz C et al. Design, synthesis and antimycobacterial activities of 1-methyl-2-alkenyl-4(1H)-quinolones. *Bioorg Med Chem* 2011; **19**: 567–79.
- 20** Evangelopoulos D, Bhakta S. Rapid methods for testing inhibitors of mycobacterial growth. In: *Antibiotic Resistance Protocols, Methods in Molecular Biology*. New York: Humana Press, 2010: 279.
- 21** Schinkovitz A, Gibbons S, Stavri M et al. Ostruthin: an antimycobacterial coumarin from the roots of *Peucedanum ostruthium*. *Planta Med* 2003; **69**: 369–71.
- 22** Wallace AC, Laskowski RA, Thornton JM. LIGPLOT: a program to generate schematic diagrams of protein–ligand interactions. *Protein Eng* 1995; **8**: 127–34.
- 23** Friesner RA, Banks JL, Murphy RB et al. Glide: a new approach for rapid, accurate docking and scoring. 1. Method and assessment of docking accuracy. *J Med Chem* 2004; **47**: 1739–49.
- 24** Cornish-Bowden A. *Fundamentals of Enzyme Kinetics*. London: Portland Press, 2004.
- 25** Adams M, Wube AA, Bucar F et al. Quinolone alkaloids from *Evodia rutaecarpa*: a potent new group of antimycobacterial compounds. *Int J Antimicrob Agents* 2005; **26**: 262–4.
- 26** Richardson JF, Reith S. Characterization of a strain of methicillin-resistant *Staphylococcus aureus* (EMRSA-15) by conventional and molecular methods. *J Hosp Infect* 1993; **25**: 45–52.
- 27** Orme I. Search for new drugs for treatment of tuberculosis. *Antimicrob Agents Chemother* 2001; **45**: 1943–6.
- 28** Drlica K, Zhao X. DNA gyrase, topoisomerase IV, and the 4-quinolones. *Microbiol Mol Biol Rev* 1997; **61**: 377–92.
- 29** Xia Y, Yang Z-Y, Morris-Natschke SL et al. Recent advances in the discovery and development of quinolones and analogues as antitumor agents. *Curr Med Chem* 1999; **6**: 179–94.
- 30** Chu DT, Fernandes PB. Structure–activity relationships of the fluoroquinolones. *Antimicrob Agents Chemother* 1989; **33**: 131–5.
- 31** Krovat EM, Steindl T, Langer T. Recent advances in docking and scoring. *Current Computer-Aided Drug Design* 2005; **1**: 93–102.
- 32** Umamaheswari A, Pradhan D, Hemanthkumar M. Virtual screening for potential inhibitors of homology modeled *Leptospira interrogans* MurD ligase. *J Chem Biol* 2010; **3**: 175–87.
- 33** Herschlag D. The role of induced fit and conformational changes of enzymes in specificity and catalysis. *Bioorg Chem* 1988; **16**: 62–96.
- 34** Pettersen EF, Goddard TD, Huang CC et al. UCSF Chimera—a visualization system for exploratory research and analysis. *J Comput Chem* 2004; **25**: 1605–12.